Modelling tools for the simulation of microgenerators based on piezo-semiconducting nanowires

Olivier Graton, Guylaine Poulin-Vittrant, Louis-Pascal Tran Huu Hue, Marc Lethiecq

ACOUSTICS 2012

Modelling tools for the simulation of microgenerators based on piezo-semiconducting nanowires

O. Graton[a], G. Poulin-Vittrant[a], L.-P. Tran Huu Hue[a] and M. Lethiecq[b]

[a]Université François Rabelais, ENIVL, Rue de la Chocolaterie, 41034 Blois, France
[b]Université François Rabelais de Tours, GREMAN, ENIVL, Rue de la Chocolaterie BP 3410, 41034 Blois, France
olivier.graton@univ-tours.fr

Novel mechanical energy micro-harvesters using ZnO nanowire (NW) arrays as active elements have recently appeared. The electrical power generation process is based on the coupling between piezoelectric and semiconducting properties of ZnO NWs. We have developed two specific models to simulate the electromechanical conversion that occurs in mechanically activated NWs and to predict the performance of NW-based microgenerators. These models, based on two distinct approaches, take into account both the piezoelectric effect and semiconducting properties of NWs. An original analytical-numerical model is dedicated to the simulation of the intrinsic electromechanical conversion that occurs in a bent NW in the presence of free charge carriers. In addition, a modelling strategy was specifically developed in order to establish a dynamic model of NW-based microgenerators without falling into the different pitfalls relative to their simulation. These two approaches are complementary and are helpful for the physical understanding of the device operation. Moreover, it indicates tendencies to optimise the generator performance.

1 Introduction

Conjugate progresses made in micro and nano-manufacturing and electronics has lead to the development of novel devices. The low power consumption of such devices make it interesting to develop autonomous systems that can harvest a part of their surrounding energy to provide for their energetic needs. Among the different sources, mechanical energy is one of the most versatile available in natural environment that can be found under the form of acoustic waves, mechanical vibrations and shocks or gas and fluid flow. Piezoelectric micro generators (PMG) seem to be good candidates to ensure the energy conversion, however typical PMGs operate at their resonant frequency and are no longer efficient outside their narrow bandwidth. Moreover, reducing the size of PMGs often leads to an increase of their operating frequency range. This could be a potential problem to efficiently harvest energy from natural sources such as wind, water waves or blood flow that are time varying low frequency sources. Recently, a new generation of micro-harvesters based on ZnO nanowires (NW) arrays have been developed with promising results [1, 2]. This kind of generator works in quasi-static regime, thus the number of active NWs rather than the operating frequency increases the amount of energy that is converted. A ZnO NW can be seen as a quasi one-dimensional nanotransducer that exhibits both piezoelectric and semiconducting properties. This particularity makes ZnO NWs not only suitable for energy harvesting, but also for sensor, actuator or electronic applications [3].

Classical models of piezoelectric converters cannot be used, especially because of the semiconducting properties of ZnO. Nevertheless, the modeling of such an electromechanical system is essential both for the physical understanding and as an optimisation tool. The purpose of this work is the development of a strategy to overcome the different pitfalls in the modeling of the electromechanical conversion in ZnO NWs. This paper focuses on a major difficulty due to the coupling between piezoelectric and semiconducting properties of the material. The free electric charges can interact with the electric field that appears in a mechanically activated NW [4]. Moreover, a NW integrated in an energy-harvesting device should have at least two electrical contacts to be connected to the external load. Depending on the metal used for the electrodes and due to the semiconducting nature of ZnO, a metal-semiconductor (MS) junction can be obtained. This junction that acts as a Schottky diode also has a strong impact on the device electrical behaviour. The establishment of the electric potential and the charge transport in a mechanically activated NW are ruled by non-linear coupled equations.

Two specific models have been developed. Thanks to an analytical-numerical approach, the electromechanical conversion of energy that occurs in a laterally deflected ZnO NW has been studied. This model is well suited for single nanostructures. In complement, the equivalent circuit of the NW seen as a metal/semiconductor/metal (MSM) structure, taking into account the piezoelectric effect has been designed. This model is multi-scale and could be adapted for single NW as well as NW-based micro-devices.

The next two sections focus on each model and discuss the main results.

2 Mixed model of the intrinsic electromechanical conversion of energy

2.1 Theoretical Background

A NW is a natural cantilever that has a hexagonal shape due to its wurtzite crystalline structure. In this approach, it is modelled as a clamped-free beam with a regular hexagonal cross-section that is statically bent by a force F applied at its free end (Fig. 1). The electrical potential Φ that appears in the bent NW is calculated in a section of the NW, taking into account the presence of free charge carriers. Here, the static electrical problem is considered, *i.e*. the NW conductivity σ is very small. In that case, Φ is ruled by the Poisson equation:

$$\varepsilon_{11}^{S}\nabla^2\phi=-(\rho_P-\rho_F) \tag{1}$$

where ρ_P is the piezoelectric charge density and ρ_F the free charge density. ε_{11}^{S} is the ZnO longitudinal dielectric permittivity.

By resolving the Saint-Venant's problem, an analytical expression of ρ_P has been established for a hexagonal cross-section NW [5]. ρ_F is the free charge in the NW. ZnO is a natural n-doped semiconductor due to defects in its crystal lattice that act like impurities. For simplicity of calculation, we consider only one shallow level donor E_{d0}=30 meV that represents interstitial Zn atoms denoted (Zn_i) [6]. ρ_F is due to the presence of free electrons in the conduction band and ionized impurities on E_{d0}:

$$\rho_F=q(N_{d^+}-n) \tag{2}$$

with q the elementary charge. Free electrons concentration n and ionized impurities concentration N_d^+ are calculated thanks to Fermi-Dirac statistics [7]:

a)

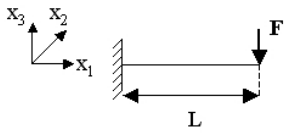

b)

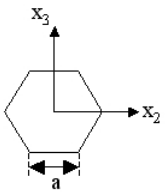

Figure 1: a) NW loaded at its free end b) NW cross-section.

$$n = N_c \exp\left(\frac{E_F - E_C}{k\Theta}\right)$$
$$N_{d+} = \frac{N_d}{1+\exp\left(\frac{E_F - E_d}{k\Theta}\right)} \quad (3)$$

where N_d is the Zn_i concentration, N_c the effective density of states in conduction band, k the Boltzmann constant, Θ the temperature and E_F the Fermi level. E_C is the conduction band edge of the NW. It is flat in the case of a non deformed NW. When the NW is bent, Φ and **T** deform the conduction band edge. This phenomenon is expressed as follows:

$$E_C = -q\phi + E_{def} \quad (4)$$

where E_{def} is the deformation potential related to the stress tensor **T** [8]. This expression is fundamental since it expresses the coupling of piezoelectric and semiconducting properties. Since ρ_F depends on Φ, (1) has a non-linear source term. It is solved thanks to the finite element method (FEM).

2.2 Results

Results shown in Fig. 2 compare the electrical potential Φ established in the half-length cross section of a lightly doped NW (N_d = 10^{10} cm^{-3}) and a moderately doped NW (N_d = 10^{17} cm^{-3}). Calculations are performed for a 1µm length and 100 nm diameter NW bent by a load F = 0.2 µN surrounded by an insulating medium (air) at room temperature (Θ = 300 K).

In the lightly doped case, Φ has a quasi-symmetric distribution, as it would be in a purely dielectric NW. The tensed side exhibits a positive potential Φ+ that reaches a maximum of 0.28 V whereas the compressed side shows a negative potential Φ- reaching – 0.28 V. In the moderately doped case, Φ is no longer symmetric and presents a maximum of only 0.04 V in the tensed side, while Φ is preserved in the compressed side.

a)

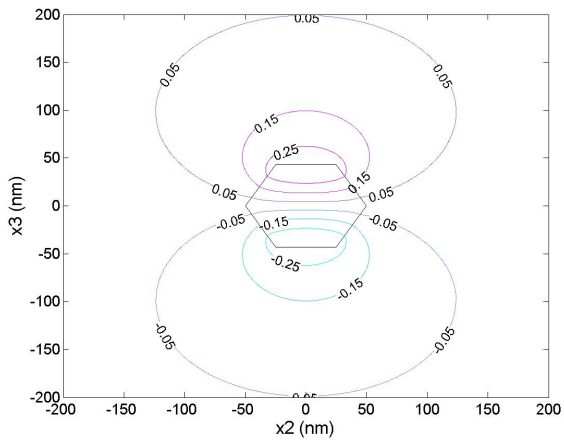

b)

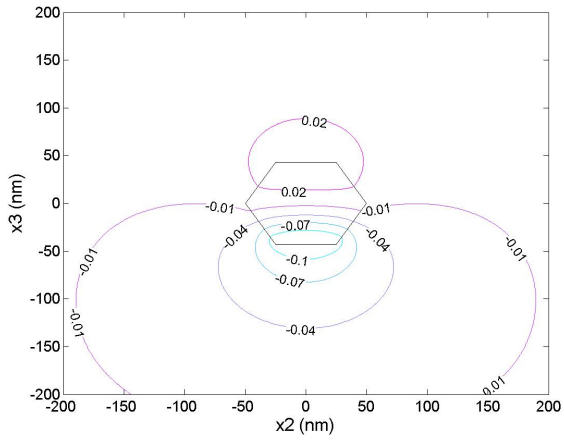

Figure 2: Electrical potential Φ in the half length cross section of a) a lightly doped NW (N_d=10^{10} cm^{-3}) b) a moderately doped NW (N_d=10^{17} cm^{-3}).

This asymmetry comes from the fact that Φ is partially screened by free charges. (4) shows that Φ+ lowers the conduction band edge E_c, whereas Φ- raises it. This has a direct impact on the repartition of the free electrons; indeed, free electrons occupy in priority lower energy levels of the conduction band. Free electrons accumulate on the tensed side of the NW, whereas the compressed side is depleted from free charge carriers. On the compressed side, Φ- is partially screened by electrical charges that come from ionised impurities N_d^+. Moreover, N_d^+ is a fixed charge. It cannot freely move in the NW and because of its shallow level E_{d0}, almost all impurities are ionised ($N_d^+ \sim N_d$).

In complement, parameters that influence Φ have been studied. One can distinguish three types of parameters: geometrical (a, L), material (N_d) and external (F, Θ). Those which have the most significant impact are NW radius a, doping N_d and applied force F.

In Fig. 3-a) and 3-b), the effect of a on Φ is represented. The other parameters are kept constant (L=1 µm, F=0.2 µN and Θ = 300 K). Fig. 3-c) and 3-d) show the effect of F on Φ, while the other parameters are kept constant (L=1 µm, a=0.05 µm and Θ = 300 K). The impact of these two parameters is illustrated for common values of doping N_d.

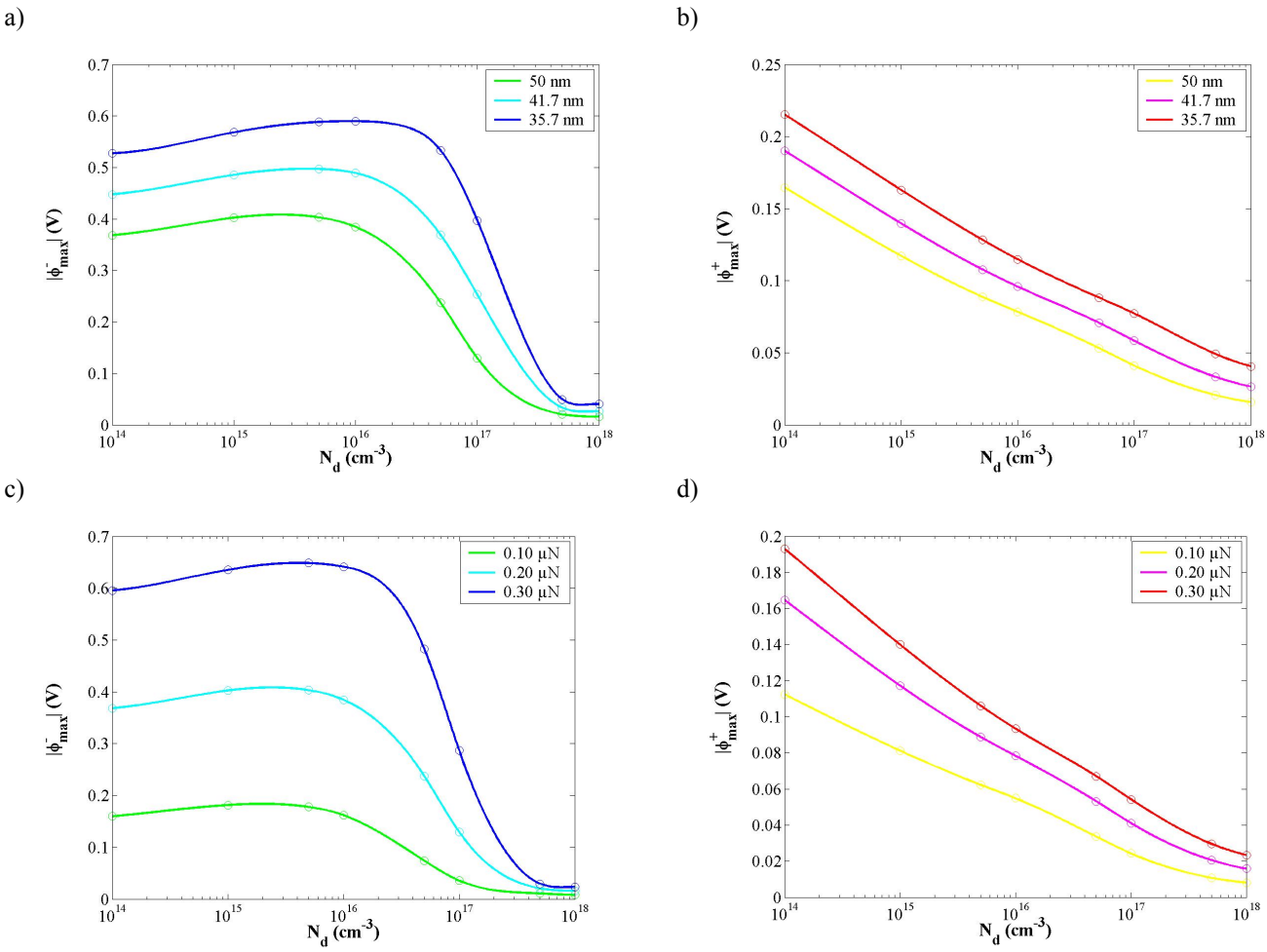

Figure 3: Effect of N_d on the maximum amplitude of Φ for a) and b) NWs with different radius a (at constant F) and for c) and d) different magnitudes of F (at constant a).

Φ increases as a decreases. It can be explained as follows: for a same applied force, stresses and strains are increased for a thinner NW thus leading to a higher ρ_P. The same phenomenon happens at constant radius when F varies (see Fig. 3-c) and 3-d)). Stresses and strains are maximised for higher magnitudes of bending force.

The impurities concentration N_d also has a strong impact on Φ. There are two extreme cases. For a highly doped crystal (N_d>10^{17} cm^{-3}), Φ vanishes as it is screened in the tensed side by free electrons and in the compressed side by ionised impurities. For low doping (N_d<10^{15} cm^{-3}), Φ is preserved in both parts of the NW and tends to the value obtained in the theoretical case of a pure crystal. For intermediate values, an interesting result is the existence of an optimal doping where $|\Phi^-_{max}|$ reaches a maximum.

This model is well suited for the study of the intrinsic electromechanical conversion that occurs in mechanically activated piezo-semiconducting nanostructures. Nevertheless, it is difficult to adapt this approach for the modeling of a whole device based on NWs arrays. Simulations of microsystems containing several tens of thousands of NWs will be time-consuming. Moreover, this model is static so it cannot predict the performance of NW based microgenerators. These pitfalls were overcome by using a lumped element model introduced in the next part.

3 Model of a nanowire based microgenerator.

The equivalent circuit of a NW working in quasi-static 33 mode is established. This model is well-adapted for sensing or energy harvesting applications in which operating frequencies are far below the resonance of the NWs, typically from DC to a few tens of kHz. Then, numerical results for different structures are presented and discussed.

3.1 Equivalent circuit

A 1D ZnO NW (length L_3 >> diameter d) shown in Fig. 4-a) in which top and bottom faces are covered by metal electrodes is considered. The axis denoted x_3 coincides with the c-axis of the ZnO crystal. A force F, along x_3 axis, is applied at the top face of the NW. A voltage V_{out} can be collected across an electrical load connected to the two electrodes. A_3 is the area of the electrode that is taken equal to the NW cross-section for the calculations. L_3 is the NW's length. The equivalent circuit of such a structure, according to [9], is presented in Fig. 4-b).

It is composed of three parts. The piezoelectric conversion is composed of a voltage source V_{33} controlled by an external force and a series capacitor C_{33}. Their expressions are given by (5) and (6) respectively with g_{33}

the piezoelectric coefficient and β^T_{33} the dielectric impermeability constant of ZnO at constant stress.

$$V_{33} = \frac{g_{33}}{\beta^T_{33} C_{33}} F \quad (5)$$

$$C_{33} = \frac{A_3}{L_3 \beta^T_{33}} \quad (6)$$

a)

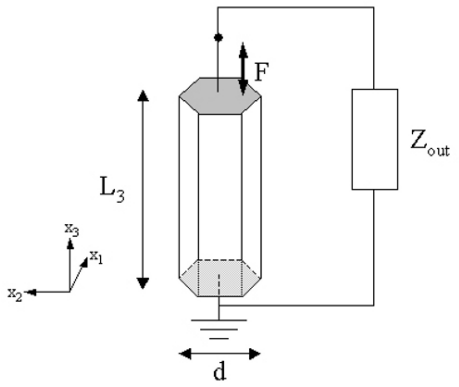

b)

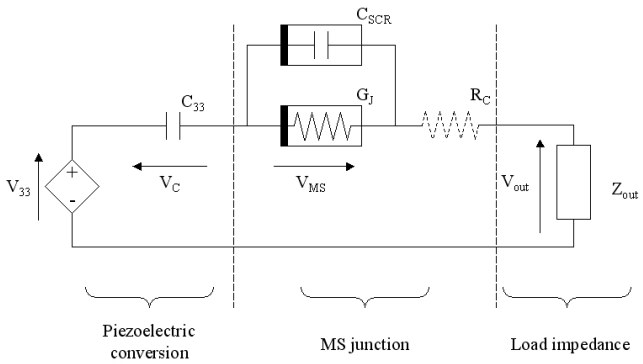

Figure 4: a) Description and b) equivalent circuit of the modeled device.

The MS junction formed between the NW and the upper electrode has two operating modes. If one applies a bias voltage $V_{MS}<V_D$ with V_D the diffusion potential of the Schottky contact, the junction is reverse-biased. A space charge region (SCR) appears where a positive charge is stored. Since V_{MS} modulates the SCR length W, the stored charge also varies with V_{MS}, which corresponds to a dynamic capacitor C_{scr} expressed by (7). The junction also has a parallel dynamic conductance G_j that represents the thermoionic current that can flow through the junction [7]. When $V_{MS} \geq V_D$, the junction is forward-biased and no longer has a capacitive effect. Only the conductive effect remains. G_j is given by the derivative of the current density J with respect to V_{MS} and is proportional to J_S the saturation current density (8) whatever the operating mode.

$$C_{scr} = A_3 \sqrt{\frac{\varepsilon_{33} q N_d}{2(V_D - V_{MS})}} \quad (7)$$

$$G_J = A_3 \frac{q J_S}{k\Theta} \exp\left(\frac{q V_{MS}}{k\Theta}\right) \quad (8)$$

3.2 Results

The following results concern a microgenerator made of one million NWs with hexagonal cross-section under a harmonic quasi-static force of magnitude 1.2 µN at a frequency of 50 Hz. NWs are connected in parallel in order to increase the current delivered by the NW array. The microgenerator performance is examined when varying two kinds of parameters: the NW's dimensions which impact energy conversion via the piezoelectric effect and the nature of the top electrode that modifies the Schottky barrier. The force magnitude is chosen to induce a maximum compressive strain of 0.1% for the thinnest NW. The choice of the electrical design and the mechanical source characteristics used in the model are inspired by results found in literature [2].

The performance of the microgenerator was evaluated when varying NW's dimensions. F is kept constant (F = 1.2 µN) and an Au electrode is used. Three different configurations are compared to study both the influence of a and L_3. The output voltage, current and power (V_{out}, I_{out}, P_{out}) delivered to an optimal resistive load (R_{opt}) are calculated as well as the microgenerator power density P_{dens} (relative to the volume of active material) that can be seen as a figure of merit of the device. Results are summarised below in Table 1.

	Config. # 1	Config. # 2	Config. # 3
L_3 (µm)	2	2	1
a (µm)	0.1	0.05	0.05
V_{out} (V_{RMS})	4.9	19.4	10.1
I_{out} (nA_{RMS})	1.94	1.86	1.86
P_{out} (nW_{RMS})	9.5	37.6	18.8
R_{opt} (GΩ)	2.5	10	5.4
P_{dens} ($mW_{RMS}.mm^{-3}$)	0.18	2.9	2.9

Table 1: Microgenerator performance for different configurations.

Configurations 1 and 2 differ in the NW radius value a, respectively 100 nm and 50 nm. L_3 is kept constant. This has an impact on both the mechanical and the electrical behaviour of the device. When the NW radius is reduced and the same force applied, the compressive strain ξ_3 increases and leads to a higher voltage V_{33} induced by piezoelectric effect, V_{33} being implicitly proportional to ξ_3. Because ξ_3 is inversely proportional to a^2, V_{33} and V_{out} are quadratically increased. Even if V_{out} increases for thinner NWs, I_{out} undergoes a small decrease. This can be explained as follows: the microgenerator can be seen as a capacitor formed by the array of NWs and the two electrodes. Then, a good approximation of the microgenerator impedance is given by $Z_{\mu G} \approx 1/(j\omega C_{33})$. By reducing a, $Z_{\mu G}$ and R_{opt} increase, thus limiting I_{out}. Nevertheless, P_{out} is multiplied by 4 and rises to 37.6 nW_{RMS} while P_{dens} is multiplied by 16 and reaches 2.9 $mW_{RMS}.mm^{-3}$.

Configurations 2 and 3 differ in the NW length L_3, respectively 2µm and 1µm. Even if it has no impact on the magnitude of compressive strain ξ_3, reducing L_3 will increase C_{33}. Because V_{33} is inversely proportional to C_{33}, both V_{33} and V_{out} decrease. In the same time, $Z_{\mu G}$ decreases, preserving I_{out}. An interesting result is that for the same NW radius, P_{dens} stays unchanged whatever the NW length. These results show that microgenerators made of the thinnest NWs have the highest power density among the three configurations presented above (P_{dens} = 2.9 $mW_{RMS}.mm^{-3}$).

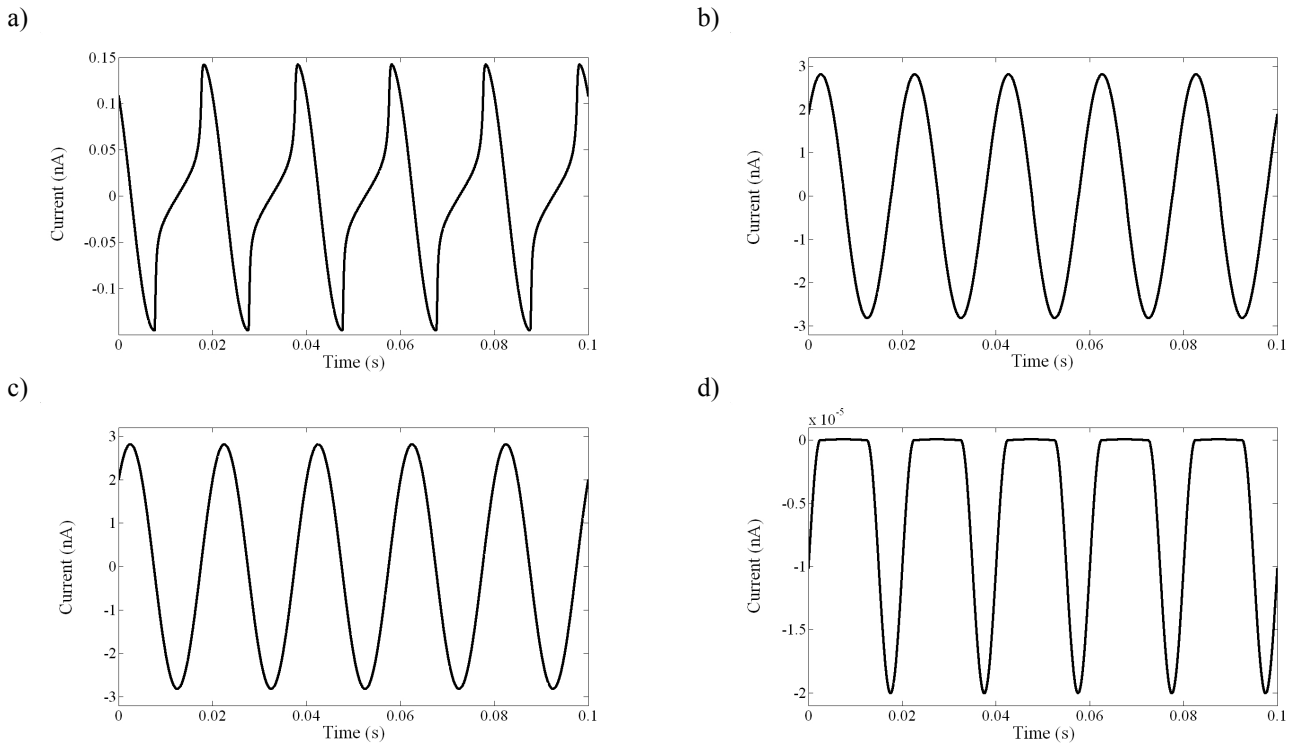

Figure 5: Current flowing through a) C_{scr} and b) G_j for a Au electrode; c) C_{scr} and d) G_j for a Pt electrode.

These results are in agreement with those found in literature [2]. Nevertheless, if reducing a improves V_{out}, it also increases $Z_{\mu G}$ thus limiting I_{out}. In the case of a low magnitude excitation ($F < 100$ nN), I_{out} will be too small to harvest a significant amount of energy. To achieve a high efficiency piezoelectric conversion, one has to come to a compromise concerning the NW dimensions. Both L_3 and a influence $Z_{\mu G}$, showing that the NW dimensions have an impact on the overall device performance.

Finally, the influence of the nature of the electrode on the microgenerator performance is studied. The chosen NW dimensions are those of configuration 2. Au and Pt electrodes that have two distinct work functions are considered ($\Phi_{M\text{-}Au} = 5.1$ eV and $\Phi_{M\text{-}Pt} = 5.65$ eV). In both cases, P_{out} reaches a value of 37.6 nW_{RMS}. P_{out} is not significantly changed by the properties of the junction. Moreover, no rectifying effect is observed on V_{out}. However, it is interesting to study in detail the current flowing through the MS interfaces, as shown in Fig. 5.

For the Au electrode, most of the current flows through G_j because the current generated by the NWs array is below the junction saturation current J_S and the conduction is rather ohmic (Fig. 5-a and 5-b). For the Pt electrode, a rectifying effect across G_j is observed. However, most of the current flows through C_{scr} (Fig. 5-c and 5-d). In this case, the use of Au electrodes makes the junction equivalent to an ohmic junction, whereas the Pt-ZnO junction has a capacitive behaviour.

4 Conclusion

In summary, we have presented two complementary approaches. The mixed model gives a support for the understanding of the intrinsic electromechanical conversion in ZnO NWs, describing in detail the distribution of the physical quantities inside the NW. The lumped element model is rather a systemic approach that studies the global behaviour and predicts the performance of NW-based microgenerators. Furthermore, the models indicate tendencies and are helpful to optimise the growth of the NWs; for example, both approaches highlight the impact of NW dimensions on electromechanical conversion. Ongoing work concerns an exhaustive parametric study of the lumped element model in order to determine the parameters that most influence the device performance.

References

[1] S. Xu et al, *Nano Lett.* 8(11), 4027-4032 (2008)

[2] G. Zhu et al., *Nano Lett*. 10, 3151-3155 (2010)

[3] S. Xu et al, *Nat. Nanotechnol.* 5, 366-373 (2010)

[4] Y. Gao and Z.L. Wang, *Nano Lett.* 9(3), 1103-1110 (2009)

[5] O. Graton et al., *Proceedings of Powermems*, Leuven, Belgique (2010)

[6] L Schmidt-Mende and J.L. MacManus-Driscoll, *Mater. Today* (10), 40-48, (2007)

[7] S.M. Sze and Kwok K. Ng, *Physics of Semiconductor Devices (3rd edition),* Wiley (2007)

[8] P.Y. Yu and M. Cardona, *Fundamentals of Semiconductors (3rd edition)*, Springer (2005)

[9] O. Graton et al, to be published in *Adv. Appl. Ceram.* (2012)